

Accelerated sea-level rise is suppressing CO₂ stimulation of tidal marsh productivity: A 33-year study

Chunwu Zhu^{1,2*}†, J. Adam Langley^{3†}, Lewis H. Ziska⁴, Donald R. Cahoon⁵, J. Patrick Megonigal^{2*}

Accelerating relative sea-level rise (RSLR) is threatening coastal wetlands. However, rising CO₂ concentrations may also stimulate carbon sequestration and vertical accretion, counterbalancing RSLR. A coastal wetland dominated by a C₃ plant species was exposed to ambient and elevated levels of CO₂ in situ from 1987 to 2019 during which time ambient CO₂ concentration increased 18% and sea level rose 23 cm. Plant production did not increase in response to gradually rising ambient CO₂ concentration during this period. Elevated CO₂ increased shoot production relative to ambient CO₂ for the first two decades, but from 2005 to 2019, elevated CO₂ stimulation of production was diminished. The decline coincided with increases in relative sea level above a threshold that hindered root productivity. While elevated CO₂ stimulation of elevation gain has the potential to moderate the negative impacts of RSLR on tidal wetland productivity, benefits for coastal wetland resilience will diminish in the long term as rates of RSLR accelerate.

Copyright © 2022
The Authors, some
rights reserved;
exclusive licensee
American Association
for the Advancement
of Science. No claim to
original U.S. Government
Works. Distributed
under a Creative
Commons Attribution
NonCommercial
License 4.0 (CC BY-NC).

INTRODUCTION

Coastal wetland plant communities including marshes, mangroves, tidal freshwater forests, and seagrasses are widely recognized as providing wildlife habitat, improved water quality, storm surge protection, and carbon sequestration. Under the relatively low rates of sea-level rise and stable environmental conditions of the Holocene, coastal wetlands have maintained elevation relative to changing sea levels through the sequestration of autochthonous carbon and trapping of allochthonous sediment (1), maintaining wetland surface elevation relative to sea level (2). However, there is evidence that climate change–driven acceleration of sea-level rise (3, 4) combined with land subsidence (5), the sum of which is relative sea-level rise (RSLR), is increasingly outpacing the rate of coastal wetland elevation gain, potentially “drowning” these important ecosystems. Some assessments indicate a potential 20 to 48% loss of estuarine marshes during the 21st century (6, 7), although these estimates remain highly uncertain due to the lack of local data and process knowledge (7, 8).

Climate change arises primarily from the infrared absorption properties of the greenhouse gas CO₂; however, increases in atmospheric CO₂ concentration can also promote plant growth by increasing the rate of photosynthesis and biomass accumulation, principally for plants with the C₃ photosynthetic pathway (approximately 90% of all plant species). Empirical studies demonstrate that projected increases in plant production in response to future elevated CO₂ concentration (eCO₂) can increase vertical accretion and elevation gain (9–11). Modeling studies forecast that this response will increase the resilience of tidal marshes to accelerated RSLR (12, 13). Because the resilience gained from the stimulatory effects of eCO₂ on plant photosynthesis and growth is projected to be substantial (12, 13), it is important to verify projections based on models with long-term (decadal scale) experimental manipulations that test

eCO₂ effects on plant production, biogenic deposition, and accretion rate. If sustained over time, eCO₂ could accelerate biomass accumulation and elevation gain, leading to enhanced resilience for C₃-dominated wetlands, including tidal marshes and mangroves (7).

Whether rising eCO₂-mediated effects on plant productivity can counterbalance RSLR over the long term (decades) is unclear. For marshes that are dominated by C₄ plants, which respond minimally to rising CO₂ concentrations (14, 15), eCO₂ is unlikely to influence resilience to RSLR. In contrast, models parameterized from the eCO₂ response of short-term experiments forecast that eCO₂ will substantially mitigate this outcome in C₃-dominated wetlands (12, 13). However, these forecasts have not considered whether the eCO₂ stimulation of plant biomass and elevation gain observed in short-term eCO₂ experiments will persist in C₃-dominated tidal wetlands under more realistic scenarios in which multiple global change factors are interacting to enhance or diminish eCO₂ stimulation of C₃ plant productivity.

In 1987, open-top chambers were established in a brackish tidal marsh on the Chesapeake Bay, USA to simulate projected (ca. 700 $\mu\text{mol mol}^{-1}$) atmospheric CO₂ concentrations (14). It is now the longest experimental study of the impacts of rising CO₂ concentration on ecosystem function. A subset of the experimental plots in the study is dominated by the North American C₃ sedge *Schoenoplectus americanus* (formerly *Scirpus olneyi*). After more than three decades, the response of the C₃ plant community to experimentally manipulated eCO₂ can be evaluated against changes in uncontrolled background environmental conditions such as slowly rising ambient CO₂ concentration, sea level, salinity, precipitation, temperature, and nitrogen loading. Sufficient time has elapsed to determine whether the projected increase in CO₂ concentration used in this study has resulted in temporal variation in the stimulation of plant biomass relative to other global change factors. This information is critical for assessing the impact of both recent and projected global change on tidal wetland ecosystem function and resilience.

RESULTS AND DISCUSSION

Absent or diminished plant responses to ambient and elevated CO₂

Ambient atmospheric CO₂ concentration increased from 348 $\mu\text{mol mol}^{-1}$ in 1987 to 410 $\mu\text{mol mol}^{-1}$ in 2019 (~18% increase), but there

¹State Key Laboratory of Soil and Sustainable Agriculture, Institute of Soil Science, Chinese Academy of Sciences, Nanjing 210008, PR China. ²Smithsonian Environmental Research Center, 647 Contees Wharf Road, Edgewater, MD 21037, USA.

³Department of Biology, Center for Biodiversity and Ecosystem Stewardship, Villanova University, 800 E. Lancaster Avenue, Villanova, PA 19805, USA. ⁴Environmental Health Science, Mailman School of Public Health, Columbia University, 722 West 168th Street, New York, NY 10032, USA. ⁵Eastern Ecological Science Center, U.S. Geological Survey, 12100 Beech Forest Road, Laurel, MD 20705, USA.

*Corresponding author. Email: cwzhu@issas.ac.cn (C.Z.); megonigalp@si.edu (J.P.M.).
†These authors contributed equally to this work.

is no evidence of a concomitant increase in *S. americanus* peak annual aboveground biomass (Fig. 1 and fig. S1). Experimental $e\text{CO}_2$, simulating end-of-century atmospheric conditions (ca. 700 $\mu\text{mol mol}^{-1}$), stimulated shoot biomass production, with considerable interannual variation related to salinity and sea level as previously reported (16, 17). However, when cumulative changes in shoot biomass are considered over the full 33-year period (to 2019), a sigmoidal function is observed, which illuminates decadal-scale variation in the plant productivity response to $e\text{CO}_2$ (Fig. 2), related primarily to the shoot density response (fig. S2).

The sigmoidal shape of the cumulative $e\text{CO}_2$ biomass response to time function indicates three distinct temporal phases in the $e\text{CO}_2$ response: An initial “lag” phase of about 4 years (1987–1990), characterized by high variability in the biomass response, may reflect plant and microbial adjustment to the sudden step increase in CO_2 concentration; a second phase (1991–2002) is characterized by a larger and more consistent $e\text{CO}_2$ stimulation of biomass (i.e., a steeper and relatively linear cumulative response); and a third phase beginning ca. 2005 when the $e\text{CO}_2$ response declined. This third phase suggests a suppression of the $e\text{CO}_2$ response due to external factors that interfere with the response, or negative feedbacks arising from the $e\text{CO}_2$ response such as acclimation or progressive N limitation.

The first two phases of the $e\text{CO}_2$ response were noted in previous syntheses of the shoot biomass data from this experiment, particularly the second phase of consistent $e\text{CO}_2$ stimulation of biomass production, consistent with that of Rasse *et al.* (18) and Erickson *et al.* (17) for data compiled through 2004. Phases 1 and 3 are apparent in the $e\text{CO}_2$ shoot biomass response data compiled by Drake (16) for this experiment through 2010, although the post-2005 decline (phase 3) was not noted. We have not observed the same patterns in a second $e\text{CO}_2$ experiment colocated at the Global Change Research Wetland (GCRW) that began in 2006 (9, 19), possibly because the strong $e\text{CO}_2$ response phase that we might have expected at the start of the newer experiment occurred at a time (i.e., post-2005) when other factors, such as accelerated RSLR, were suppressing the $e\text{CO}_2$ responses, as observed in the older experiment. Our analysis of the full 33-year record demonstrates that the

response of *S. americanus* biomass to $e\text{CO}_2$ has declined significantly since 2006 (Fig. 3).

Environmental drivers of diminished plant $e\text{CO}_2$ response

The decline in plant biomass response to $e\text{CO}_2$ that began after ca. 18 years of treatment does not correspond to temporal patterns in several factors known to regulate primary productivity in tidal marshes such as annual precipitation or average growing season salinity in the adjacent estuary or soil porewater (fig. S3). Maximum growing season air temperature declined by ca. 3°C from 1987 to 2019, but minimum air temperature increased by 5°C with no net effect on average air temperature (fig. S4). Although nitrogen (N) limits plant growth responses to $e\text{CO}_2$ at this site (20, 21), there were no temporal trends in concentrations of dissolved $\text{NO}_3^- + \text{NO}_2^-$, dissolved NH_4^+ , or particulate-bound NH_4^+ in the Rhode River sub-estuary adjacent to the study site (fig. S5). There were also no temporal trends in shoot or above ground N content within CO_2 concentration treatments (fig. S6). There were $e\text{CO}_2$ -driven differences in tissue N content, but these differences were consistent throughout the study, even when $e\text{CO}_2$ stimulation of biomass varied temporally (fig. S6). We did not quantify changes in suspended sediment because sediment deposition on the upland edge of this high marsh where the experiment is located is negligible as illustrated by the fact that soil organic matter content is >80% (19).

Relative sea level was the only temporal variable in our analysis that corresponded to declining trends in the *S. americanus* shoot biomass response to $e\text{CO}_2$. When the shoot biomass response to $e\text{CO}_2$ is binned in 2-year increments to account for lags in plant response and plotted against growing season sea level (when these plant species are photosynthetically active), there is a nonlinear relationship (Fig. 4). $e\text{CO}_2$ initially stimulated productivity when sea level was below an elevation of ca. 15 cm with respect to the North American Vertical Datum of 1988 (NAVD88), but above this elevation threshold, $e\text{CO}_2$ stimulation declined. This elevation threshold corresponds closely to marsh surface elevation at this site of 20- to 25-cm NAVD88 (22). Because root productivity at the site also began to decline above the 15-cm NAVD88 threshold (Fig. 4), we

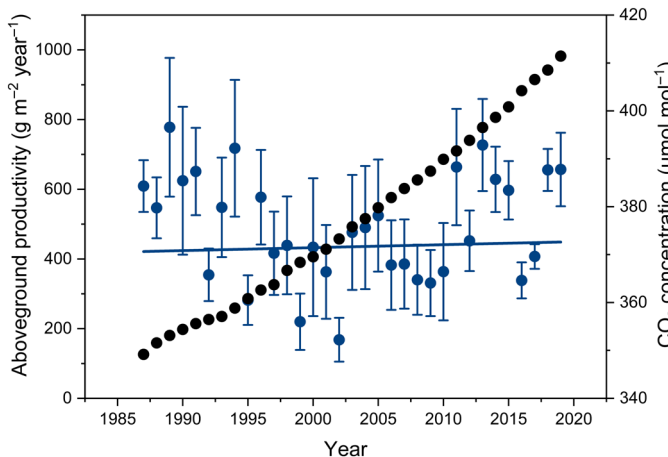


Fig. 1. Ambient CO_2 and shoot biomass. Peak annual aboveground biomass ($\pm\text{SE}$) of the C_3 sedge *S. americanus* from 1987 to 2019 in chambered plots at ambient CO_2 concentration (left axis, blue symbols), during which ambient CO_2 concentration rose from 348 to 410 $\mu\text{mol mol}^{-1}$ (black symbols, right axis). No significant changes in biomass were observed ($P = 0.72$). The blue line is the best-fit linear regression result ($R^2 = 0.004$, $P = 0.72$).

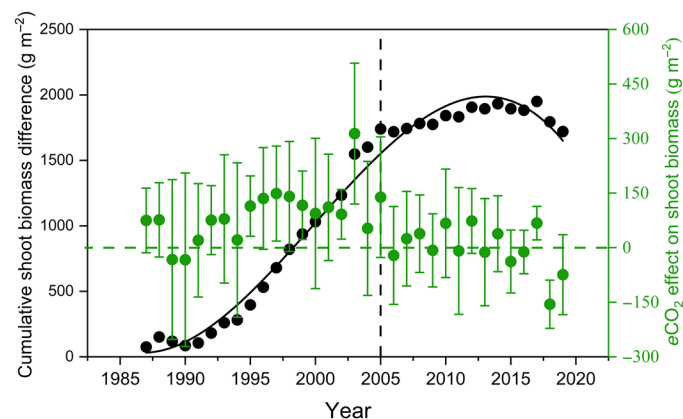


Fig. 2. Shoot biomass responses to $e\text{CO}_2$. Shoot biomass responses to $e\text{CO}_2$ exposure from 1987 to 2019 plotted as both the annual difference in the mean biomass of the elevated (E) and ambient (A) treatments (right y axis in green symbols) and the cumulative difference in mean biomass of the two treatments over time (left y axis in black symbols). Cumulative shoot biomass data were fit to years of treatment with a fourth-order quadratic equation ($Y = 1170 + 3850X - 930X^2 - 826X^3 + 343X^4$, $R^2 = 0.99$, $P < 0.001$).

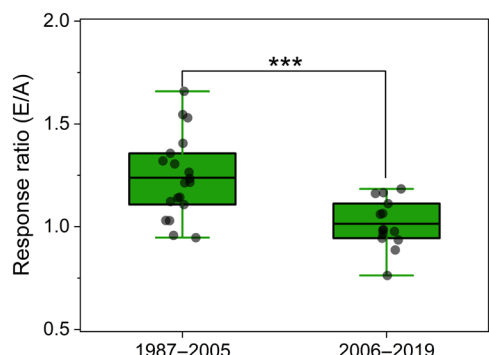


Fig. 3. Early and late phases of eCO₂ responses. The eCO₂ response ratio of *S. americanus* biomass in the plant community dominated by *S. americanus* from 1987 to 2005 compared to 2006 to 2019. The response ratio was calculated as annual mean biomass at eCO₂ (E) divided by the annual mean biomass at ambient CO₂ (A). Symbols represent a significant difference between the two groups at $P < 0.001$ (**). The response ratio from 1987 to 2005 was significantly different from 1.0 ($P < 0.001$), while the response ratio from 2006 to 2019 was not significantly different from 1.0 ($P = 0.669$).

infer that increasing periods of soil saturation caused the diminished eCO₂ response. The increase in sea level was accompanied by a minor decrease in tidal range (fig. S7). This may have increased the duration of marsh inundation over time (23, 24) but was likely too small to be important.

Mechanisms for sea level–driven loss of eCO₂ stimulation

The extent to which sea-level rise translates into increased flooding frequency at our tidal marsh study site depends on rates of deep land subsidence and the rate of soil surface elevation gain. The study site is in a region of rapid deep subsidence that exacerbates the increase in flooding caused by sea-level rise alone (5, 25). This loss of elevation can be offset by plant-driven elevation gain, a process that eCO₂ can stimulate (9). Although we do not have changes in soil elevation data before 2005 for this experiment, the total elevation gain since 2005 at an adjacent experiment was 2.2 cm at ambient CO₂ and 3.8 cm at eCO₂ (2005–2019; Fig. 5), far less than the ca. 15-cm increase in sea level during the same period (Fig. 6). Thus, eCO₂ stimulation of elevation gain was not rapid enough during a 14-year period in the adjacent experiment to offset the increase in flooding frequency inferred from local RSLR. Further evidence of an increase in the rate of RSLR at the site is a clear shift in plant community composition to more flood-tolerant species (i.e., *S. americanus*) over the past decade, as this site has become more frequently inundated (26).

We propose that increasing inundation caused by RSLR crossed a physiological threshold in approximately 2005, whereby flooding began to interfere with the ability of *S. americanus* to respond to eCO₂. Although the specific physiological basis for an RSLR-driven reduction in eCO₂ response is unclear, our results suggest that the mechanism relates to flooding effects that begin with impacts on belowground production. In previous work at this site and elsewhere, flooding stress reduces root-to-shoot ratio of plant production (27), a response that is directly opposed to one of the most consistent plant responses to eCO₂, which is increased growth allocation to roots (28). In the present study, root production declined sharply across both treatments as eCO₂ stimulation of aboveground production declined (Figs. 4 and 6). Inundation frequency and

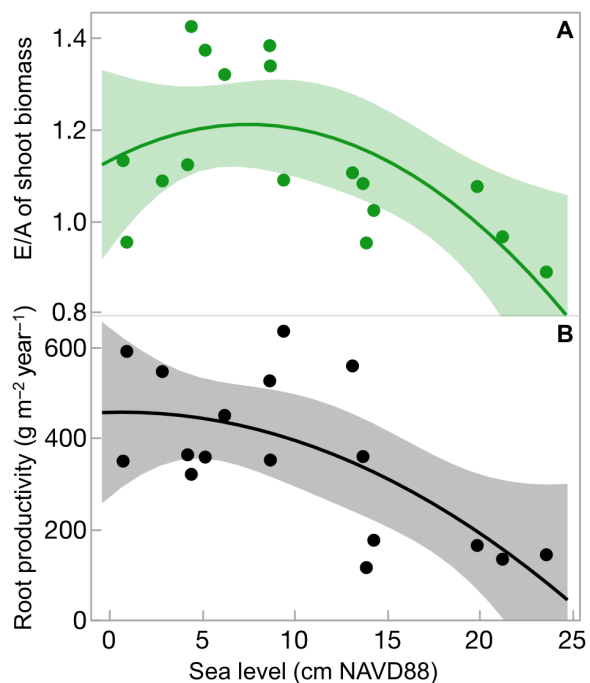


Fig. 4. Shoot biomass eCO₂ response to sea level. (A) Relationship between sea level and shoot biomass response ratio to eCO₂ for *S. americanus* (top). Replicates in a CO₂ concentration treatment were averaged in 2-year intervals beginning from 1987 to account for lags between sea-level change and plant production responses to sea level. The shoot biomass response ratio is the ratio of the 2-year averages for the eCO₂ (E) and ambient CO₂ (A) treatments. (B) Relationship of root productivity to sea level. Root productivity in each 2-year interval is the average of the eCO₂ and ambient CO₂ treatments. Lines represent quadratic fits: $E/A = 1.131 + 0.0213 \times SL - 0.000141 \times SL^2$ ($R^2 = 0.388$, $P = 0.032$); root productivity = $455.9 + 1.007 \times SL - 0.715 \times SL^2$ ($R^2 = 0.449$, $P = 0.016$). Shading encompasses the 95% confidence interval of the quadratic relationship. SL, sea level.

duration increased as RSLR accelerated, which likely caused higher anaerobic stress in roots, increased concentrations of toxins such as sulfide, and reduced photosynthetic capacity due to nitrogen limitation (29–31). We suspect that flooding stress precluded shifting plant allocation patterns that are commonly observed in relatively low-stress conditions to help sustain eCO₂ stimulation of productivity, including enhancing nutrient foraging (32) and a belowground growth sink for photosynthates, without which eCO₂ stimulation of photosynthesis can decline due to acclimation (33). Thus, plant growth stimulation in response to eCO₂ is subordinate to the strict physiological limitations imposed by flooding.

Implications for tidal wetland resilience

Declining root productivity and the declining eCO₂ effect on aboveground biomass may portend a decline in aboveground biomass productivity in this marsh. In a previous sea-level manipulation, we found that the optimum elevation for root production lies higher than the optimum elevation for aboveground production (27). This pattern may explain why root productivity has declined sharply without a concomitant decline in aboveground production so far (Figs. 1 and 4). We predict that the rate of RSLR will continue to outpace the rate of elevation gain at this site, which currently lies below mean growing season sea level (Figs. 5 and 6), and that aboveground plant growth will decline in the coming decades.

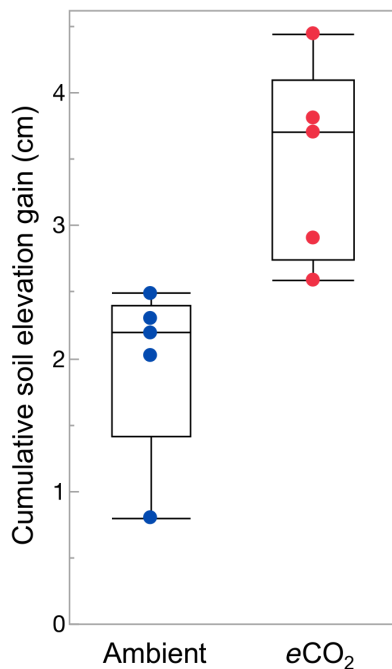


Fig. 5. Cumulative surface elevation gain. Cumulative elevation gain for *S. americanus*-dominated plots from 2006 to 2019 for ambient (A) and elevated (E) CO₂ treatments. Elevation measurements were made in a companion experiment colocated at the study site that began in 2006 (7). The increase in elevation for both CO₂ treatments is significantly less than the long-term rate of sea-level rise (3.7 mm year⁻¹) in the 93-year record from the Annapolis NOAA gauge. Elevation change was measured with a modified surface elevation table [(9, 41); table S1].

Accelerating RSLR may also explain why the slow increase in ambient CO₂ concentration over 33 years has not increased plant production in the ambient treatment. Another possibility is that rising CO₂ concentration was sufficiently gradual as to allow for photosynthetic acclimation; this acclimation has been observed in *Arabidopsis* with gradual CO₂ concentration increases over multiple generations (34). In our field study, a sharp step increase in CO₂ concentration to simulate end-of-century concentrations did significantly increase shoot biomass (following a brief lag phase) for over a decade (Figs. 2 and 3), showing that the eCO₂ stimulation observed in short-term eCO₂ studies can persist over decades. However, in this instance, the eCO₂ stimulation of biomass was transient at a decadal scale because of a negative feedback imposed by accelerating RSLR.

Previous research in a companion experiment at this location that began in 2006 indicated that future eCO₂ concentrations could increase soil volume and elevation gain in the short term (2 years) (9) due primarily to enhanced rates of root production. Numerical models have forecast that the eCO₂ response will improve tidal marsh resilience in C₃-dominated marshes if maintained over decades (12, 13). However, the current study suggests that gradual increases in ambient atmospheric CO₂ concentration over a 33-year period were insufficient to stimulate biomass production, and that the larger stimulatory benefits of future CO₂ concentrations for plant biomass and soil elevation gain could diminish over time as rates of RSLR accelerate. This pattern is consistent with the reduction in root production over time observed here (Figs. 4 and 5). The slightly higher elevation of the eCO₂ treatment predicted by the

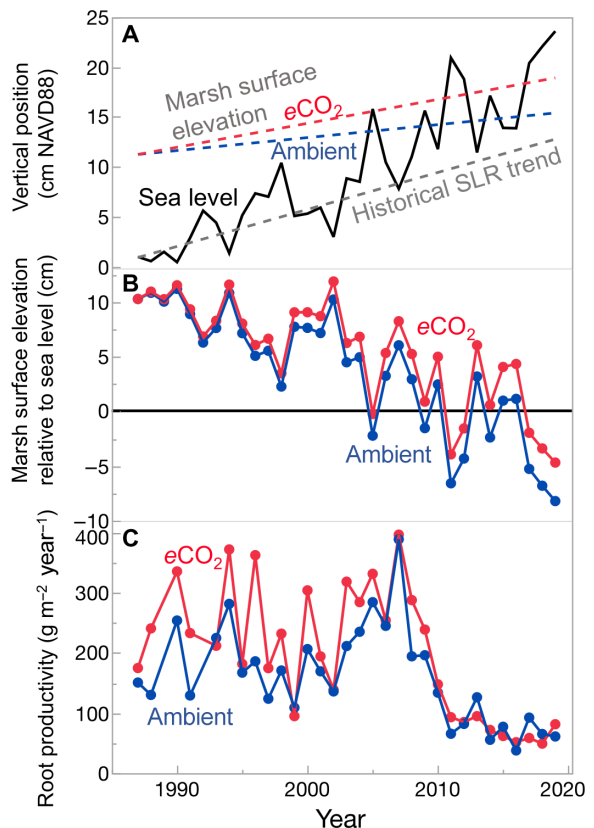


Fig. 6. Elevation trends in relation to root production. (A) Absolute elevations of marsh plots and sea level. Marsh elevations are based on elevation surveys and elevation change estimates modeled from an adjacent eCO₂ experiment, yielding rates for eCO₂ (red dashed line) and ambient CO₂ (blue dashed line) plots. The sea-level trace (black line) represents annual mean sea level for each growing season (May to July) from the Annapolis gauge. The historical rate of sea-level rise based on a linear fit of the 93-year record from the Annapolis NOAA gauge (3.7 mm year⁻¹, dashed gray line) is plotted at the same starting point for comparison to the actual mean sea level over the interval of this study, 1987–2019. (B) Estimated marsh elevations relative to sea level for eCO₂ (red symbols) and ambient CO₂ (blue symbols). In a given year, marsh elevations below 0 are lower than sea level during the growing season. (C) Root productivity in eCO₂ (red symbols) and ambient (blue symbols) plots over 33 years.

model after ca. 2006 when root productivity in the two treatments converged (Fig. 4) is likely an overestimate arising from our assumption that eCO₂ stimulation of elevation measured over 14 years in the 2006 experiment applied linearly over the 33 years of 1987 experiment. However, even this best-case scenario does not allow the marsh to increase elevation at the rate of sea-level rise.

Although the potential for rapid RSLR to suppress eCO₂ stimulation of plant production should, in principle, apply widely to coastal wetland ecosystems based on known physiological limits to flood tolerance, the likelihood and timing of such a response depends on many factors. Key plant traits such as flood tolerance, salinity tolerance, and eCO₂ stimulation of photosynthesis can determine physiological thresholds. For example, invasive genotypes of *Phragmites australis* respond to eCO₂ and other climate change factors differently from native species, which may promote relatively higher rates of elevation gain (35, 36). Conversely, any stimulatory effect of eCO₂ on *Rhizophora* spp. production, a C₃ mangrove tree species,

may be short term and dependent on low-salinity conditions and species type (37, 38). The current study was conducted in a sediment-limited geomorphic setting, negating the potential for *eCO₂* to stimulate soil elevation gain through increased sediment deposition (21, 27), suggesting that *eCO₂* stimulation of elevation gain could be more persistent in systems with high suspended sediment concentrations. Other plant traits and hydrogeomorphic conditions influenced by climate change such as lateral migration and resistance to erosion need additional clarification as to their impact on wetland functionality (39). However, it must be acknowledged that the interactions of *eCO₂* and other global change factors are certain to alter wetland plant community composition and biogeochemistry with consequences for ecosystem resilience to RSLR.

Overall, the future ecological function of coastal wetlands will depend on the interactions of RSLR and several physical, hydrological, and biological processes that determine resilience via soil elevation gain and tidal wetland migration into uplands. On the basis of short-term responses, it has been proposed that increasing atmospheric CO₂ concentration, by stimulating plant productivity, will enhance soil elevation gain and increase tidal wetland resilience to RSLR in C₃-dominated systems (9–11). While additional data for other coastal wetland ecosystems are urgently needed, the current study synthesized the longest continuous (33-year) record of current and future CO₂ concentration effects on a C₃ plant community to conclude that marsh inundation frequency will cross a critical threshold at which RSLR and flooding stress overcomes the stimulatory effect of *eCO₂* on *S. americanus* biomass production. We conclude that *eCO₂* cannot be assumed to significantly enhance wetland resilience to RSLR in the long term. Further work is required to refine the mechanisms by which RSLR suppresses *eCO₂* stimulation of plant growth and identify the biohydrogeomorphic conditions that govern this response.

MATERIALS AND METHODS

Site description

The experiments were conducted at GCReW, a facility of the Smithsonian Environmental Research Center (Edgewater, MD, USA). GCReW occupies a large portion of Kirkpatrick Marsh (38°53'N, 76°33'W), a 22-ha site on the Rhode River, a microtidal sub-estuary of the Chesapeake Bay. Large areas of the site are dominated by a C₃ sedge, *S. americanus* (previously described as *S. olneyi*), and two C₄ perennial grasses, *Spartina patens* and *Distichlis spicata*, which are widely distributed as monocultures and mixtures in tidal brackish marshes throughout the eastern seaboard and Gulf of Mexico coast of the United States. All three species have perennial roots, rhizomes, culms, and annual shoots. Soils at the site are highly organic (>80% organic matter) to a depth of ca. 5 m. At the time the primary experiment was initiated (May 1987), mean tidal range was 44 cm and the high marsh zone where the experiment is located was ca. 40 to 60 cm above daily mean low water level (22). In summer 2021, the elevation of the experimental plots in the primary study averaged 17.7 cm (\pm SD 3.0 cm) NAVD88.

Experimental design

Open-top chambers in the primary experiment were installed in May 1987 to expose aboveground biomass to elevated atmospheric CO₂ concentrations *in situ* (40). The original chambers were 1.2 m tall and 0.8 m in diameter and encompassed 0.47 m² of the soil

surface (40). The full study design includes ambient and *eCO₂*-treated plots in each of three distinct plant communities, but the data in the present study are from the *S. americanus*-dominated community only, as *eCO₂* effects in the other two plant communities are confounded by the presence of C₄ species that do not respond strongly to *eCO₂*. Five chambers in the *S. americanus* community were ventilated with ambient air that was ca. 348 $\mu\text{mol mol}^{-1}$ in 1987 and ca. 410 $\mu\text{mol mol}^{-1}$ in 2019. An additional five chambers were ventilated with ambient air amended with an additional ca. 340 $\mu\text{mol mol}^{-1}$ CO₂, representing an approximate doubling of CO₂ concentration relative to 1987 levels. The *eCO₂*-treated chambers received supplemental CO₂ by continuous injection of 100% CO₂ gas into the input blower, where it mixed with ambient air before being circulated into the chamber via a second blower and manifold. This chamber design was modified in 2014 to eliminate the second blower such that the ambient air mixed with CO₂ entered the manifold directly, similar to the design of Langley *et al.* (41). The dimensions of the chambers did not change in 2014 other than an increase in area from 0.47 to 0.53 m² due to a change in chamber shape from circular to octagonal.

A second experiment began in 2006 that crossed *eCO₂* and supplemental nitrogen (41). The 2006 study is dominated by *S. americanus*, located 10 to 100 m from the 1987 study, and has an elevation range similar to the *S. americanus*-dominated plots in the 1987 study. The open-top chambers are very similar to the 1987 study in design but enclose seven times more soil surface area (3.3 m²) and are fitted with surface elevation tables for tracking changes in soil surface elevation.

Biomass determination

Shoot density, growth, and aboveground biomass were estimated annually for each plot from 1987 to 2019. The total number of *S. americanus* shoots was manually counted at the peak of the growing season at the end of July or early August (42). Allometric models were developed from linear regressions of oven-dry stem mass to stem diameter and height as determined by the harvest of stems from each plot annually from 1987 to 2016 (42). Stem density was determined for each plot by counting stems in the entire 0.47-m² plot area. Aboveground biomass was calculated as the product of mean individual plant biomass from the allometric equations and plant density. Root biomass productivity was assessed annually by three replicate ingrowth bags deployed in late autumn in each plot (17). Bags were recovered the following autumn, and contents were sorted into roots and rhizomes, oven-dried, and weighed. Root production is presented here on a soil surface area basis and does not include rhizomes, which are poorly sampled by this method. Samples of dry shoots were analyzed for C and N concentrations at the Smithsonian Stable Isotope Laboratory (Suitland, MD, USA) or the UC Davis Stable Isotope Facility (Davis, CA, USA).

Marsh elevation measurement

Elevation history of plots in the 1987 experiment was approximated from elevation measurements in the adjacent companion experiment that began in 2006 (9). The 2006 experiment is a cross between *eCO₂* and added nitrogen, but data were used only from the subset of plots that did not receive nitrogen. Elevation in the 2006 experiment was measured using a modified surface elevation table (9, 41). Briefly, a stainless steel rod was driven into the soil to the point of refusal (ca. 7 m) in each plot to establish a stable benchmark. An

aluminum beam was affixed to the benchmark, extended horizontally through the chamber and an adjacent unchambered plot, and leveled precisely to occupy the same reference plane in space during each sampling. Fiberglass pins (6.35 mm diameter) of known length were placed through holes at 4-cm intervals in the beam and gently lowered to the soil surface so that the 40 to 50 pins within each chamber landed on the same point of the marsh surface during each sampling. The height of each pin relative to the benchmarked and leveled beam was recorded to the nearest millimeters at each measurement time point. Measurements were made at least twice each year except for the period 2012–2019 when there was a technical issue with the measurements. Cumulative elevation change was calculated as the product of the average annual rate of elevation change (see the “Statistical analysis” section) and the total duration of the time series (14 years; fig. S8 and table S1). The 33-year elevation history of plots in the 1987 experiment was approximated by assuming that all plots had the same initial elevation at the start of the study, and they gained elevation at a constant rate equal to their respective treatments (ambient CO₂ or eCO₂) in the 2006 experiment.

Environmental and nutrient data

Trends in variables that are known to influence tidal wetland primary productivity came from several sources. Data on salinity in Rhode River water that inundates the marsh were collected at a fixed location and depth located 1.6 km from Kirkpatrick Marsh (table S2) using three different instruments as explained by Gallegos *et al.* (43). Porewater salinity was calculated from [Cl⁻] on triplicate samples per chamber drawn from 20-cm depth as described by Keller *et al.* (44). Depth-integrated concentrations of dissolved NO₃⁻ + NO₂⁻, dissolved NH₄⁺, and particulate-bound NH₄⁺ in the Rhode River (table S3) were determined within 100 m of Kirkpatrick Marsh [station 5T in (44)] from 1986 to 2019 following the methods of Correll *et al.* (45). Points are annual averages of 20 to 38 observations from 1986 to 2011 and 6 to 19 observations thereafter.

Precipitation and temperature data are from the iAIMS Climatic Data repository for the U.S. Naval Academy at Annapolis, Anne Arundel County, MD, USA, station “Annapolis US NAVAL ACA” (<https://beaumont.tamu.edu/climaticdata/WorldMap.aspx>), located 11 km from Kirkpatrick Marsh. Mean sea-level data are reported as mean water level at a National Oceanic and Atmospheric Administration (NOAA)/National Ocean Service (NOS) tide gauge relative to the NAVD88 datum. Mean hourly water level data from 1987 to 2019 were averaged each year for the months of May, June, and July. The data were obtained from the U.S. Naval Academy at Annapolis, MD, station 8575512 (https://tidesandcurrents.noaa.gov/sltrends/sltrends_station.shtml?id=8575512).

Annual averages of environmental and nutrient variables were calculated for the full year or the growing season depending on the relationship of the variable to eCO₂ effects on primary production. Sea level, salinity, precipitation, and temperature were summarized for May, June, and July. We define the growing season as starting in May when green shoots emerge from the soil and ending in July when plant biomass peaks, and we conduct a field assessment of annual aboveground biomass production. The growing season technically extends through October, but we cannot quantify the effects of environmental variables on shoot biomass production past July. In addition, the effects of sea level, salinity, precipitation, and temperature on plant growth during the remainder of the year (August onward)

are less important than during the main growing season. In contrast, nitrogen inputs to the marsh in the nongrowing season accumulate in soils and can affect growing season primary productivity; therefore, we averaged nitrogen concentrations for the full annual record.

Statistical analysis

Linear regression relationships between time and environmental variables were conducted using SigmaPlot (Statview Software, Cary, NC, USA), JMP (JMP Pro, Cary, NC, USA), or OriginPro version 2021b (OriginLab Corporation, Northampton, MA, USA). The fourth-order quadratic in Fig. 2 was calculated in OriginPro version 2021b. Differences in the *S. americanus* biomass eCO₂ response ratio for the periods 1987–2005 and 2006–2019 were determined by a two-sample *t* test applied to the means between the two groups, and a one-sample *t* test to compare whether the means of each group were significantly different from 1.0 using R (46). Rates of elevation gain were calculated for each individual measurement pin as the slope of all elevation measurements versus time; this approach avoids over-weighting any one elevation time point, which is subject to tidal and seasonal fluctuations. Next, the slopes of individual pins were averaged to generate a mean elevation change for each plot. Last, ambient CO₂ and eCO₂ treatments were compared by *t* test (*n* = 5). We tested for chamber effects on *S. americanus* shoot biomass by comparing ambient plots with and without chambers. We applied a two-way repeated-measures analysis of variance (ANOVA) with year as the within-subject factor and CO₂ concentration as the between-subject factor using bruceR (47). Because this test showed a significant Treatment × Year interaction, we used post hoc *t* tests to identify years with significant differences. Statements about the absence of statistical significance are based on *P* < 0.05. Standard error of the mean (SEM) for the eCO₂ effect on shoot biomass (Fig. 2) was calculated as

$$\sqrt{(\text{SEM ambient})^2 + (\text{SEM elevated})^2}$$

SUPPLEMENTARY MATERIALS

Supplementary material for this article is available at <https://science.org/doi/10.1126/sciadv.abn0054>

REFERENCES AND NOTES

1. K. Rogers, J. Kelleway, N. Saintilan, J. P. Megonigal, J. B. Adams, J. R. Holmquist, M. Lu, L. Schile-Beers, A. Zawadzki, D. Mazumder, C. D. Woodroffe, Wetland carbon storage controlled by millennial-scale variation in relative sea-level rise. *Nature* **567**, 91–95 (2019).
2. M. L. Kirwan, J. P. Megonigal, Tidal wetland stability in the face of human impacts and sea-level rise. *Nature* **504**, 53–60 (2013).
3. S. Hofer, C. Lang, C. Amory, C. Kittel, A. Delhasse, A. Tedstone, X. Fettweis, Greater Greenland Ice Sheet contribution to global sea level rise in CMIP6. *Nat. Commun.* **11**, 6289 (2020).
4. R. M. Deconto, D. Pollard, Contribution of Antarctica to past and future sea-level rise. *Nature* **531**, 591–597 (2016).
5. R. S. Nerem, T. M. Van Dam, M. S. Schenewerk, Chesapeake Bay subsidence monitored as wetlands loss continues. *Eos Trans. AGU* **79**, 149–157 (1998).
6. C. Craft, J. Clough, J. Ehman, S. Joye, R. Park, S. Pennings, H. Guo, M. Machmuller, Forecasting the effects of accelerated sea-level rise on tidal marsh ecosystem services. *Front. Ecol. Environ.* **221**, 73–78 (2009).
7. M. L. Kirwan, S. Temmerman, E. E. Skeehan, G. R. Guntenspergen, S. Fagherazzi, Overestimation of marsh vulnerability to sea level rise. *Nat. Clim. Change* **6**, 253–260 (2016).
8. J. R. Holmquist, L. N. Brown, G. M. MacDonald, Localized scenarios and latitudinal patterns of vertical and lateral resilience of tidal marshes to sea-level rise in the contiguous United States. *Earth's Future* **9**, e2020EF001804 (2021).
9. J. A. Langley, K. L. McKee, D. R. Cahoon, J. A. Cherry, J. P. Megonigal, Elevated CO₂ stimulates marsh elevation gain, counterbalancing sea-level rise. *Proc. Natl. Acad. Sci. U.S.A.* **106**, 6182–6186 (2009).

10. J. A. Cherry, K. L. McKee, J. B. Grace, Elevated CO₂ enhances biological contributions to elevation change in coastal wetlands by offsetting stressors associated with sea-level rise. *J. Ecol.* **97**, 67–77 (2009).
11. R. Reef, T. Spencer, I. Möller, C. E. Lovelock, E. K. Christie, A. L. McIvor, B. R. Evans, J. A. Tempest, The effects of elevated CO₂ and eutrophication on surface elevation gain in a European salt marsh. *Glob. Chang. Biol.* **23**, 881–890 (2017).
12. K. M. Ratliff, A. E. Braswell, M. Marani, Spatial response of coastal marshes to increased atmospheric CO₂. *Proc. Natl. Acad. Sci. U.S.A.* **112**, 15580–15584 (2015).
13. A. J. Rietl, J. P. Megonigal, E. R. Herbert, M. L. Kirwan, Vegetation type and decomposition priming mediate brackish marsh carbon accumulation under interacting facets of global change. *Geophys. Res. Lett.* **48**, e2020GL092051 (2021).
14. P. S. Curtis, B. G. Drake, P. W. Leadley, W. J. Arp, D. F. Whigham, Growth and senescence in plant communities exposed to elevated CO₂ concentrations on an estuarine marsh. *Oecologia* **78**, 20–26 (1989).
15. S. F. Jones, C. L. Stagg, K. W. Krauss, M. W. Hester, Flooding alters plant-mediated carbon cycling independently of elevated atmospheric CO₂ concentrations. *J. Geophys. Res. Biogeosci.* **123**, 1976–1987 (2018).
16. B. G. Drake, Rising sea level, temperature, and precipitation impact plant and ecosystem responses to elevated CO₂ on a Chesapeake Bay wetland: Review of a 28-year study. *Glob. Chang. Biol.* **20**, 3329–3343 (2014).
17. J. E. Erickson, J. P. Megonigal, G. Peresta, B. G. Drake, Salinity and sea level mediate elevated CO₂ effects on C₃–C₄ plant interactions and tissue nitrogen in a Chesapeake Bay tidal wetland. *Glob. Chang. Biol.* **13**, 202–215 (2007).
18. D. P. Rasse, G. Peresta, B. G. Drake, Seventeen years of elevated CO₂ exposure in a Chesapeake Bay Wetland: Sustained but contrasting responses of plant growth and CO₂ uptake. *Glob. Chang. Biol.* **11**, 369–377 (2005).
19. M. A. Pastore, J. P. Megonigal, J. A. Langley, Elevated CO₂ and nitrogen addition accelerate net carbon gain in a brackish marsh. *Biogeochemistry* **133**, 73–87 (2017).
20. J. A. Langley, J. P. Megonigal, Ecosystem response to elevated CO₂ levels limited by nitrogen-induced plant species shift. *Nature* **466**, 96–99 (2010).
21. M. Lu, E. R. Herbert, J. A. Langley, M. L. Kirwan, J. P. Megonigal, Nitrogen status regulates morphological adaptation of marsh plants to elevated CO₂. *Nat. Clim. Change* **9**, 764–768 (2019).
22. J. R. Holmquist, L. Schile-Beers, K. Buffington, M. Lu, T. J. Mozdzer, J. Riera, D. E. Weller, M. Williams, J. P. Megonigal, Scalability and performance tradeoffs in quantifying relationships between elevation and tidal wetland plant communities. *Mar. Ecol. Prog. Ser.* **666**, 57–72 (2021).
23. M. L. Kirwan, G. R. Guntenspergen, Influence of tidal range on the stability of coastal marshland. *J. Geophys. Res.* **115**, F02009 (2010).
24. D. J. Coleman, M. Schuerch, S. Temmerman, G. Guntenspergen, C. G. Smith, M. L. Kirwan, Reconciling models and measurements of marsh vulnerability to sea level rise. *Limnol. Oceanogr. Lett.* **7**, 140–149 (2022).
25. A. Sallenger, K. Doran, P. Howd, Hotspot of accelerated sea-level rise on the Atlantic coast of North America. *Nat. Clim. Change* **2**, 884–888 (2012).
26. J. R. Gabriel, J. Reid, L. Wang, T. J. Mozdzer, D. F. Whigham, J. P. Megonigal, J. A. Langley, Interspecific competition is prevalent and stabilizes plant production in a brackish marsh facing sea level rise. *Estuar. Coasts* (2022).
27. J. A. Langley, T. J. Mozdzer, K. A. Shepard, S. B. Hagerty, J. P. Megonigal, Tidal marsh plant responses to elevated CO₂, nitrogen fertilization, and sea level rise. *Glob. Chang. Biol.* **19**, 1495–1503 (2013).
28. M. Nie, J. Bell, S. Raul, E. Pendall, Altered root traits due to elevated CO₂: A meta-analysis. *Global Ecol. Biogeogr.* **22**, 1095–1105 (2013).
29. P. M. Bradley, J. T. Morris, Influence of oxygen and sulfide concentration on nitrogen uptake kinetics in *Spartina alterniflora*. *Ecology* **71**, 282–287 (1990).
30. C. N. Janousek, C. Mayo, Plant responses to increased inundation and salt exposure: Interactive effects on tidal marsh productivity. *Plant Ecol.* **214**, 917–928 (2013).
31. T. D. Colmer, L. A. J. Voesenek, Flooding tolerance: Suites of plant traits in variable environments. *Funct. Plant Biol.* **36**, 665–681 (2009).
32. M. L. Kirwan, G. R. Guntenspergen, Feedbacks between inundation, root production, and shoot growth in a rapidly submerging brackish marsh. *J. Ecol.* **100**, 764–770 (2012).
33. W. J. Arp, Effects of source-sink relations on photosynthetic acclimation to elevated CO₂. *Plant Cell Environ.* **14**, 869–875 (1991).
34. N. Teng, B. Jin, Q. Wang, H. Hao, R. Ceulemans, T. Kuang, J. Lin, No detectable maternal effects of elevated CO₂ on *Arabidopsis thaliana* over 15 generations. *PLOS ONE* **4**, e6035 (2009).
35. F. Eller, C. Lambertini, L. X. Nguyen, H. Brix, Increased invasive potential of non-native *Phragmites australis*: Elevated CO₂ and temperature alleviate salinity effects on photosynthesis and growth. *Glob. Chang. Biol.* **20**, 531–543 (2014).
36. J. S. Caplan, R. N. Hager, J. P. Megonigal, T. Mozdzer, Global change accelerates carbon assimilation by a wetland ecosystem engineer. *Environ. Res. Lett.* **10**, 1150060 (2015).
37. D. R. Cahoon, K. L. McKee, J. T. Morris, How plants influence resilience of salt marsh and mangrove wetlands to sea-level rise. *Estuaries Coasts* **44**, 883–898 (2021).
38. M. C. Ball, M. J. Cochrane, H. M. Rawson, Growth and water use of the mangroves *Rhizophora apiculata* and *R. stylosa* in response to salinity and humidity under ambient and elevated concentrations of atmospheric CO₂. *Plant Cell Environ.* **20**, 1158–1166 (1997).
39. D. M. FitzGerald, Z. Hughes, Marsh processes and their response to climate change and sea-level rise. *Annu. Rev. Earth Planet. Sci.* **47**, 481–517 (2019).
40. P. W. Leadley, B. G. Drake, Open top chambers for exposing plant canopies to elevated CO₂ concentration and for measuring net gas exchange. *Vegetatio* **104**, 3–15 (1993).
41. J. A. Langley, M. V. Sigrist, J. Duls, D. R. Cahoon, J. C. Lynch, J. P. Megonigal, Global change and marsh elevation dynamics: Experimenting where land meets sea and biology meets geology. *Smithsonian Contrib. Marine Sci.* **38**, 391–400 (2009).
42. M. Lu, J. S. Caplan, J. D. Bakker, J. A. Langley, T. J. Mozdzer, B. G. Drake, J. P. Megonigal, Allometry data and equations for coastal marsh plants. *Ecology* **97**, 1–354 (2016).
43. C. L. Gallegos, T. E. Jordan, S. S. Hedrick, Long-term dynamics of phytoplankton in the Rhode River, Maryland (USA). *Estuaries Coasts* **33**, 471–484 (2010).
44. J. K. Keller, A. A. Wolf, P. B. Weisenhorn, B. G. Drake, J. P. Megonigal, Elevated CO₂ affects porewater chemistry in a brackish marsh. *Biogeochemistry* **96**, 101–117 (2009).
45. D. L. Correll, T. E. Jordan, D. E. Weller, Transport of nitrogen and phosphorus from Rhode River watersheds during storm events. *Water Resour. Res.* **35**, 2513–2521 (2009).
46. R Core Team, *R: A Language and Environment for Statistical Computing* (R Foundation for Statistical Computing, 2021); www.r-project.org/.
47. H. W. S. Bao, bruceR: Broadly useful convenient and efficient R functions. R Package Version 0.8.2 (2021); <https://CRAN.R-project.org/package=bruceR>.

Acknowledgments: We gratefully acknowledge T. Jordan for assistance with water quality data records, the enduring contributions of B. Drake who started and supervised the experiment from 1987 to 2009, the essential assistance of G. Peresta who has managed the study site since 1990, D. Peresta who manages the annual plant census, M. Lu who helped data curation, L. Song and W. Wei who helped with the data analysis and figure design, and hundreds of employees and volunteers who collected data over 33 years. Any use of trade, product, or firm names is for descriptive purposes only and does not imply endorsement by the U.S. government. **Funding:** This study was supported by Chinese Academy of Sciences “0-1” program grant ZDBS-LY-DQC020 (C.Z.); Department of Energy Terrestrial Ecosystem Science program grants DE-FG02-97ER62458 and DE-SC0008339 (J.P.M.); National Science Foundation Long-Term Research in Environmental Biology program grants DEB-0950080, DEB-1457100, DEB-1557009, and DEB-2051343 (J.A.L. and J.P.M.); U.S. Geological Survey Global Change Research Program G10AC00675 (J.P.M.); Chinese Academy of Sciences Youth Innovation Promotion Association Member No. 201957 (C.Z.); and The Smithsonian Institution. **Author contributions:** Conceptualization: J.P.M., D.R.C., and J.A.L. Methodology: J.P.M., D.R.C., and J.A.L. Investigation: J.A.L., J.P.M., and D.R.C. Data curation: C.Z., L.H.Z., J.A.L., and J.P.M. Formal analysis: C.Z., L.H.Z., J.A.L., and J.P.M. Supervision: J.P.M. and J.A.L. Writing—original draft: C.Z., J.A.L., J.P.M., and L.H.Z. Writing—review and editing: C.Z., J.A.L., J.P.M., L.H.Z., and D.R.C. **Competing interests:** The authors declare that they have no competing interests. **Data and materials availability:** Data on peak annual biomass, stem density, root productivity, and tissue N content for the primary experiment that began in 1987 are available at <https://serc.si.edu/gcrew/CO2data>. Precipitation and temperature data are available from the U.S. Naval Academy at Annapolis, MD, USA, at <https://beaufort.tamu.edu/climaticdata/WorldMap.aspx>. Sea-level data are available from NOAA at https://tidesandcurrents.noaa.gov/sltrends/sltrends_station.shtml?id=8575512, which is station 8575512 at the U.S. Naval Academy at Annapolis, MD, USA. All other data are available in the main text or the Supplementary Materials.

Submitted 27 October 2021

Accepted 1 April 2022

Published 18 May 2022

10.1126/sciadv.abn0054